LAWRENCE
LIVERMORE
NATIONAL
LABORATORY

UCRL-JRNL-203490

Corrosion Behavior of Medium Carbon Steel in Simulated Concentrated Yucca Mountain Waters

Ahmet Yilmaz, Dhanesh Chandra, Raul B. Rebak

April 13, 2004

Metallurgical and Materials Transactions A

09 April 2004
Paper prepared for publication in the Metallurgical and Material Transactions Journal as Proceedings from the symposium Effect of Processing on Materials Properties for Nuclear Waste Disposition held in Chicago on 10-11 November 2003

Corrosion Behavior of Medium Carbon Steel in Simulated Concentrated Yucca Mountain Waters.

A. Yilmaz, D. Chandra, and R.B. Rebak.*
Lawrence Livermore National Laboratory, Energy and Environment Directorate Livermore, CA 94550
**University of Nevada Reno, Metallurgical & Materials Sci. & Eng.Reno NV 89557*

Abstract

Medium carbon steel (MCS) is the candidate material for rock bolts to reinforce the borehole liners and emplacement drifts of the proposed Yucca Mountain (YM) high-level nuclear waste repository. Corrosion performance of this structural steel -AISI 1040- was investigated by techniques such as linear polarization, electrochemical impedance spectroscopy (EIS), and laboratory immersion tests in lab simulated concentrated YM ground waters. Corrosion rates of the steel were determined for the temperatures in the range from 25^{o}C to 85^{o}C, for the ionic concentrations of 1 time (1X), 10 times (10X), and hundred times (100X) ground waters. The MCS corroded uniformly at the penetration rates of 35-200 μm/year in the de-aerated YM waters, and 200-1000 μm/year in the aerated waters. Increasing temperatures in the de-aerated waters increased the corrosion rates of the steel. However, increasing ionic concentrations influenced the corrosion rates only slightly. In the aerated 1X and 10X waters, increasing temperatures increased the rates of MCS significantly. Inhibitive precipitates, which formed in the aerated 100X waters at higher temperatures (65^{o}C and up) decreased the corrosion rates to the values that obtained for the de-aerated YM aqueous environments. The steel suffered pitting corrosion in the both de-aerated and aerated hot YM environments after anodic polarization.

Introduction

Yucca Mountain (Nevada) is being characterized as the site for geological disposal of commercial nuclear spent fuel and some other forms of high-level nuclear waste in the United States. Yucca Mountain is located about 160 km northwest of Las Vegas in the state of Nevada

on land owned by the federal government [1]. The overall strategy in isolating high-level nuclear waste is to make use of the natural barriers present in the host geologic site along with the construction of a series of engineered barriers. The current waste package design consists of two concentric metal containers. The outer container would be made of a Ni-22Cr 13Mo-3W Alloy 22 (N06022), which is among the most corrosion resistant of all engineering materials. The purpose of this outer container is to provide protection against corrosion. The inner container would be thicker and made of nuclear grade type 316L stainless steel (S31603). The intended purpose of the inner barrier is to provide shield for radiation and mechanical integrity. The engineering barrier design also includes a detached drip shield that would be emplaced above the waste package to deflect any falling water or rocks from the walls of the emplacement onto the containers. The proposed material for the drip shield is Titanium Grade 7 or UNS R52400 [2].

Carbon steel was an earlier candidate for the container material for the mostly oxidizing Yucca Mountain environment. This is not longer the case; however, the characterization of the corrosion behavior of carbon steels in Yucca Mountain type environments is important since other components (e.g. rock bolts, tunnel ribs, borehole liners, inverts for container pedestal, etc.) in the drifts may still be constructed using carbon steels. Carbon steel and low alloy steels are still candidate materials for the container materials of other countries, where the emplacement environment is predicted to have a reducing redox potential [3].

The corrosion rates of carbon steels, low alloy steels and stainless steels were measured by weight loss at 100°C in both J-13 water and steam by McCright and Weiss [4]. All tested materials had lower corrosion rates in steam than in water, especially for the longer testing times. After 30 weeks of testing, the corrosion rate of 1020 carbon steel in J-13 water at 100°C was approximately 27 µm/year in water and 13 µm/year in steam. The corrosion rate of stainless steels in the same conditions was almost negligible, even for those with only 9% chromium such as 9Cr1Mo Alloy Steel. The effect of irradiation on the rate was also studied by McCright and Weiss. Under irradiated conditions the corrosion rates were higher when the rocks were present in the tested environment. It was explained that the production of oxygen and hydrogen peroxide might have increased the corrosion rate of the tested materials [4]. Corrosion rates by weight loss

of carbon steel, cast iron and alloy steel in air saturated J-13 water were measured by McCright and Weiss in the temperature range of 50°C to 100°C for 1500 h. Results showed that for all the alloys a maximum corrosion rate was reached in the 70°C to 80°C and decreased at 100°C. This could be related to the amount of dissolved oxygen in the tested electrolyte. At 100°C the corrosion rate of 1020 carbon steel, gray cast iron and 2.25Cr1Mo alloy steel was approximately 300 µm/year; however, for 9Cr1Mo alloy steel was only 7 µm/year. Carbon steel 1020 was also investigated regarding the effect of water vapor or relative humidity (RH) on its corrosion behavior at 65°C (Gdowski and Estill 1996). It was determined that an RH between 75% to 85% is necessary before 1020 carbon steel suffered any obvious corrosion damage [5].

The corrosion rate of 1016 low carbon steel was also measured in concentrated J-13 type waters (Table 2) using electrochemical techniques (Lian and Jones 1998) [6]. The corrosion rate was always below 10 µm/year for all the tested waters at the temperatures of 25°C, 50°C, 70°C and 90°C. Only in dilute aerated water (10X J-13) the corrosion rate of the carbon steel was higher than 10 µm/year. Cragnolino et al. published a comprehensive review of the corrosion modes of carbon steels regarding nuclear waste disposal evaluating the different degradation modes such as microbial influenced corrosion (MIC), general corrosion, localized corrosion and environmentally assisted cracking (Cragnolino et al. 1998) [7]. The corrosion behavior of A516 carbon steel was studied at 25°C, 65°C and 95°C in solutions containing different levels of carbonate/bicarbonate and chloride (Brossia and Cragnolino 1999) [8]. It was found that one of the most important parameters controlling the mode and rate of corrosion were pH and the ratio of chloride to total carbonate [8].

The objective of the current work was to investigate the effect of temperature and solution concentration on the corrosion behavior of the rock bolt steel in the simulated YM environments.

Experimental

Test Cells

A typical one-liter glass resin flask corrosion cell was used for the linear polarization and electrochemical impedance spectroscopy tests. A constructed Teflon lid allowed the entire cell

elements to be inserted into the solution with good sealing. Epoxy molded cylindrical specimen seen in Figure 1 was used as working electrode with 1cm^2 circular surface area exposed to the test solutions. As the counter electrode, a large (~10 cm2) platinum sheet was sealed on a glass capillary to supply good current distribution in the electrolyte. The Luggin capillary was connected to the Ag/AgCl reference electrode outside the cell via a salt bridge (Saturated KCl). The tip of the Luggin probe was always maintained the same distance (1mm) from specimen surface by means of a non-obstructing Teflon spacer in between to eliminate Luggin probe distance effects. A sealed glass capillary was used as thermo-well for controlling the temperature of the test solutions. A fritted glass capillary was used for continuous aeration/de-aeration of the solution throughout the experiments at the rate of 150 mL/min. A water-cooled condenser minimized the solution loss due to evaporation at high temperatures, while its outlet was connected to a gas trap for a better sealing against oxygen leaks. An electric mantle heater surrounded the test cell and a PID temperature controller maintained the desired temperatures in the accuracy of 0.1^{o}C. The overall construction required a minimum of glassblowing and met the specifications of ASTM standard G5.

Immersion corrosion experiments were carried out with a one-liter glass reaction flask with four-hole glass lid sealed on by O-rings. Inserted glass-blown stop joints held the fabricated glass capillary specimen hangers (hooks made of glass), purging tube, thermometer, and glass tube thermo-well on the lid. Coupon specimens were hanged in different positions in the cell: one was totally immersed, one partially immersed and, one was kept well over the solution. The same heating mantle, temperature controller, and condenser were used as in the electrochemical tests for high temperature dipping experiments. Aeration was maintained by purging air into the solution continuously at the rate of 150 mL/min. The cell design met the specifications of ASTM Standard G31.

YM water spray tests were conducted in the environmental cabinets, Standard Salt & Fog Chambers of Auto-Technology Inc., applying modified procedures of ASTM B117 for YM water spray.

Specimen Preparation

Specimens were received from the YM site as 1-inch diameter rock bolts of the chemical composition given in Table 1. Cylindrical specimens of 1cm^2 cross section with 5mm height were machined out of the rock bolts. Each specimen was mounted in epoxy resin with a thick electrical connection wire extended out of the rubber mold. After the resin became firm around the cylindrical specimen the mold was removed and specimen was ground until exposing the 1-cm2 circular surface areas. Then the manual surface grinding was continued with successive finer SiC emery papers until 600 grit finish. Prepared specimens were degreased with acetone and washed with tap water without rubbing the surface. Then they were rinsed with alcohol and distilled-de-ionized water, and immediately immersed in to the preconditioned test solution by the purged gases. The specimens were reground and reused until their seal with epoxy was broken by crevice formations.

Lab immersion and YM spray specimens have been machined out of rock bolts and I-beams in the form of coupons without causing any heating of the steels, as required by the related standards of ASTM G31 and G85. Surface grinding was done manually prior to immersion with successive finer SiC emery papers from 240 to 600-grit finish.

Solution Preparation

The test solution (1X YM water) of chemical composition given in Table 2 was prepared by mixing the formulated appropriate chemicals with distilled de-ionized water that initially kept at 35^{o}C. In formulating 10X and 100X waters overall ionic species were increased as 10 and 100 times respectively, and prepared by the same way of the 1X waters. In a couple of hours after the preparation, some insoluble chemicals were accumulated in the bottom of the solution flask. The solutions were taken out over the precipitates and filtered by No.52 filter paper to remove insoluble solutes, ending up a clear colorless water solution. Initial pH of the solutions was measured around 7.0 for 1X and 10X YM waters, and 8.2, as slightly alkaline for 100X waters.

Test Procedures

Electrochemical tests were conducted at a computer-controlled workstation loaded with potentiostats and commercial software. Simulated solutions in the test cells were conditioned (de-aerated/aerated) by continuous purging of a proper gas (nitrogen/oxygen) for two hours, before specimen immersion. Then freshly finished wet-ground specimens with the final 600-grit emery paper were immersed in to the conditioned solutions. Specimens were kept in the conditioned waters for two hours until reaching a stable open circuit potential (corrosion potential, or E_{corr}). A large sheet (15-cm^2 surface area) of platinum as a counter electrode and a salt bridge overcame possible noise and instabilities on measurements, associated with low solution concentration at the temperatures of 65^oC and 85^oC. Potentiodynamic scans were started with 300 mV cathodic over potential and they were raised linearly from there with the rate of 0.166 mV/s. The scans were extended beyond the breakdown potential regions until currents reached to 100 mA/cm^2. Potentiodynamic linear polarization method [9] (ASTM G59) was used to determine polarization resistance (Rp) values by selecting the linear portions of the polarization curves (E vs. I) within 25 mV anodic and cathodic over potentials. Then corrosion rates were calculated out of those Rp values, which are inversely proportional to the rates.

Electrochemical impedance spectroscopy [9,10] (ASTM G106) was conducted at E_{corr} using the same software and the cell set-up introduced for the polarization studies above. Rp values were determined from the real axis intercepts of the depressed semicircles of Nyquist plots [10,11].

Laboratory immersion corrosion testing of medium carbon steel rock bolt was carried out in 1X YM water at the temperatures of 25^{o}C and 75^{o}C, following the standard procedures of ASTM G31. The coupon sizes were 40.0x17.5 mm for RT, and 25x13x0.5 mm for 75^{o}C tests. Weight loss values for RT experiments were recorded approximately in weekly periods and for the 75^{o}C tests roughly at every 48-hour exposure period, in which the coupon specimens were located in different positions in the cells. Total immersion, partial immersion and non-immersion (keeping the specimen right above test solution, in the upper humid air portion) were applied at 75^{o}C, while only total immersion for the RT tests. Aeration of high temperature experiments was maintained by purging air in to the test solution continuously with constant rate of 150 mL/min throughout the tests. The time for specimen cleaning and weight loss measurements did not exceed 5 minutes during the data taking processes. Constantly flowing cold water (~14^{o}C) was introduced through the condenser, in order to minimize the solution loss due to evaporation at these elevated temperatures.

Standard ASTM G85 procedures were applied for dilute (1X) YM water spray tests. The same exposure chamber of ASTM B117 (Salt Spray Test) was employed for YM water fog testing.

Results and Discussion

Corrosion Behavior in De-aerated YM waters by polarization

All simulated concentrated solutions were colorless and clear before the specimens were dipped for conditioning. Specimens were held in the electrolytes for around two hours until reaching a stabilized E_{corr} before conducting the polarization resistance (PR) scans. No corrosion was observed on the specimens during the two-hour conditioning period in the de-aerated waters. Potentiodynamic polarization resistance method [9] was used to determine the corrosion rates of MCS in the simulated YM environments of 1X, 10X, and 100X concentrations at the temperatures of 25^{o}C, 45^{o}C, 65^{o}C, and 85^{o}C. Polarization curves for the 1X waters at high temperatures obtained with this particular method had some noise due to low ionic conductivity of the solution. However, they were smoothed out by the features of the software before the Rp and corrosion rate calculations.

Linear polarization behavior of MCS in 1X YM water given in Figure 2 shows the differences in both, cathodic and anodic regions for the test temperatures of 25^{o}C and 85^{o}C. Each linear portion of the cathodic branches (Tafel Lines) intercepted different current values (I_{corr}) at the corrosion potential (E_{corr}). This result revealed corrosion rate increase with increasing temperatures from 25^{o}C to 85^{o}C. The increasing temperatures also increased the passive current density in the anodic region, as shown in Figure 2. The passive regions became vertical straight lines when temperature was raised to 85^{o}C, suggesting that the dissolved oxygen amount in the electrolyte was at a minimum at 85^{o}C, as oxygen solubility is reduced at higher temperatures [11]. The breakdown potential (BP) decreased with increasing temperatures from 25^{o}C to 65^{o}C, however it increased again at 85^{o}C. This effect may have been caused by the inhibition of chloride attack [11], by the formed extra anions at ~85^{o}C in the test solution. This increase in BP at 85^{o}C was mostly observed with the dilute waters (1X, 10X). Corrosion currents of all test concentrations (1X, 10X and 100X) in the de-aerated waters were close to each other, as shown in Figure 3. The polarization technique showed that the concentration change in the ionic content from 1X to 100X influenced corrosion of MCS slightly at each fixed temperature. Figure 3 shows that the anodic region of the polarization is not affected by water concentration, but in the cathodic region the current density seemed to increase as the ionic concentration increased. The I_{corr} values and corrosion rates determined by linear polarization technique for the de-aerated environments from 25^{o}C to 85^{o}C are given in Table 3. The corrosion rates are between 35 μm/year and 168 μm/year for the various ionic concentrations in the investigated temperature range.

As a complementary technique, electrochemical impedance spectroscopy (EIS) was conducted to confirm the trends of corrosion rates determined by the linear polarization method. Observations showed that EIS had a better sensitivity to the corrosion rates for the electrolytes of low conductivity such as 1X and 10X waters. The results of EIS experiments for de-aerated waters conducted at E_{corr} are shown with Nyquist plots in Figures 4 and 5. The results of EIS showed the same corrosion rate trends for MCS, as in the linear polarization tests. Polarization resistance Rp for each environment is represented with the diameters of the depressed semicircles, which are inversely proportional to the corrosion rates. The EIS trends of 1X YM water at the test

temperatures given in Figure 4 are in good agreement with the polarization scanning results given in Figure 2. EIS shown in Figure 5 revealed more observable trends for those different concentrations, due to its higher sensitivity to the rates. EIS experiments for the de-aerated solutions given in Figure 5 showed slight increase in the corrosion rates with increasing concentrations.

The corrosion rates given in Figure 6, calculated from the potentiodynamic polarization resistance experiments, show an increase in the corrosion rate with the increasing temperatures for the de-aerated 1X, 10X and 100X YM waters. At the lower temperatures, there was a slight rate difference associated with electrolyte concentration, but this difference disappeared at temperatures higher than 45^{o}C. The activation energy of the corrosion reactions for the de-aerated simulated waters (considering the all test temperatures and concentrations) was calculated to be 18 kJ/mol, and was slightly lower than that for the aerated environments.

Pitting of MCS was observed in almost the entire temperature range in the de-aerated waters. Passive films that formed over the specimens were colorless and brittle, as generally associated with dielectric types. The pit formations shown in Figure 8 are nearly round in shape and distributed uniformly over the surface of all specimens, which could be attributed to a fairly uniform thickness of the surface film and its homogeneity. Visual and microscopic examinations showed that MCS in the YM aqueous environments was prone to localized corrosion such as pitting and crevice corrosion in the studied temperature range.

Corrosion Behavior in Aerated YM Waters by Polarization

The MCS specimens during the two-hour preconditioning were partly corroded in concentrated aerated hot (65^{o}C and 85^{o}C) waters before the actual polarization scans started. They did not show any corrosion product in the dilute solutions in this period at the lower temperatures such as 25^{o}C and 45^{o}C. In aerated 1X and 10X YM waters the corrosion rates increased as temperature increased (Figure 7). However, the rates for all temperatures were significantly higher in the aerated conditions. Slopes of the corrosion rate curves for 1X and 10X were also higher, as shown in Figure 7. The corrosion rates extended from 120 μm/year to the 1000

μm/year with in the studied temperature range. Since the aeration of the solutions was intentionally maintained by purging oxygen, it revealed the high corrosion rate limits for MCS in these simulated environments. Activation energy for the corrosion processes in the aerated environments was determined as 30 kJ/mol, which is approximately 1.5 times higher than that of the de-aerated environments.

In the 100X YM water the dependence between corrosion rate and temperature was different from for the 1X and 10X concentrations. In this particular environment the polarization scans revealed an increase in corrosion rates from 25^{o}C to 45^{o}C, then showed a decrease after 45^{o}C through 65^{o}C, reaching the lowest value at 85^{o}C. The data for the 100X aerated water given in Figure 7 was repeated several times with other temperature sets, and maximum corrosion rate value was always found to be at 45^{o}C. Observed precipitations and pitting over the specimens at 65^{o}C and 85^{o}C confirmed the protective film formations, which caused reduction of the rates in the aerated hot YM waters. The lower oxygen solubility at the higher temperatures may have also been a contributing factor on the decrease of corrosion rates. The precipitate scales shown in Figure 9 were white in color, and relatively thicker and smoother than the films formed in de-aerated waters (Figure 8). The pit formations in the aerated hot waters are shown in details in Figure 9. The diagonally aligned inclusions in the given micrograph are the sites where the deterioration has just started on the MCS (innermost, elliptically shaped dark portions of the pit). Results show that the MCS was prone to pitting and other localized corrosion attacks at the inclusions under the tested conditions. The light gray section in Figure 9 is the precipitation layer over the metal, and the dark gray is the corroded MCS. The white spots accumulated around the pits are the salt islands. The calculated corrosion currents and penetration rates for the MCS in aerated YM waters are given in Table 4.

Corrosion Behavior by Immersion Tests

Corrosion rates determined by basic immersion tests were in close agreement with the rates of the electrochemical tests. The mass loss measurements of MCS at room temperature shown in Figure 10, which conducted in ambient conditions for 107-day exposure period, revealed a rate of ~45 μm/year for the fully dipped MCS coupon specimens in the simulated 1X waters. This

rate is comparable with the results of electrochemical studies for the 1X de-aerated waters. The linear decay of the mass loss data shown in Figure 10 reveals that the corrosion rate of MCS did not change in the tested time interval. The corrosion rates were found to be higher in the aerated 1X YM waters at 75^{o}C. The data for the various dipping positions of the coupon specimens for 500-hour exposure is normalized and given in Figure 11. The weight loss measurements revealed corrosion rates, which were in close agreement with the electrochemical test results. Partially immersed specimens in the aerated waters had the highest rates around 1000μm/year. Since the concentration cell effects [12,13] at the solution lines are mostly responsible for this type of immersion, the higher rates for the aerated environments were expected. Non-immersed specimens (right above the water level, in the humid portion of the cell) had a rate of 510 μm/year, and the totally immersed ones had nearly 200 μm/year, which again matched closely with the potentiodynamic polarization results (Table 4) in the same environment.

Corrosion Behavior by YM Water Spray Tests

One week exposure of MCS to the sprayed 1X YM waters at 35^{o}C revealed an average rate of ~800 μm/year. These rates were fairly close to the rates of partial immersion, which is the most severe position for the dipping tests. This rate was close to the linear polarization results of the aerated dilute waters (1X and 10X) at 65^{o}C. The mass loss data of MCS in the Sprayed 35^{o}C 1X YM water is given in Figure 12. The coupon specimens after completion of the tests showed partly corroded sections while some parts of them still clear and shiny, as shown in Figure 13. MCS suffered a non-uniform corrosion in the sprayed YM water with the presence of large domains of anodic and cathodic reaction sites. These results suggested that the concentration cell effect [13] was very much in control for YM water spray tests in dilute waters. The rates determined by the partial immersion tests were closely matched to that of the modified salt spray technique, which also confirmed the domination of concentration cell effects.

By the recent work, the corrosion rate of rock bolt steel (Table 1) was shown to be low, generally below 1000 μm/year (40 mpy), or 1mm/year even in fully oxygenated conditions. Under moist conditions (vapor) corrosion rate was 200μm/year (8 mpy). These results are comparable to the

corrosion rates obtained by previous researchers in other types of carbon steels intended to be used for other applications in Yucca Mountain [4,6,8].

Conclusions

- The corrosion rate of MCS (rock bolt steel) in general increased with increasing temperatures for the de-aerated and the dilute (1X and 10X) aerated simulated electrolyte.
- MCS had lower corrosion rate in the de-aerated simulated YM waters than in the aerated ones. The rates in the de-aerated environments were determined to be between 35 μm/year and 200 μm/year in the temperature range from 25^{o}C to 85^{o}C.
- In the de-aerated waters, concentration changes in ground waters from 1X to 100X changed the corrosion of the steel only slightly.
- In the aerated 1X and 10X waters, there was a slight influence of the concentration change on the corrosion of the steel. The rates were between 124 μm/y and 1100 μm/year in the temperature range from 25^{o}C to 85^{o}C.
- The 100X aerated ground waters showed a different effect with increasing temperatures. Protective scales at the temperatures higher than 45^{o}C reduced the corrosion rate of MCS significantly.
- MCS was susceptible to localized corrosions such as pitting and crevice corrosion in the studied environments.
- The complementary EIS experiments, Lab immersion corrosion tests, and YM water spray test results were in close agreement with the potentiodynamic polarization rate results for the MCS rock bolt in the simulated concentrated YM ground waters.

Acknowledgements

This work was partially supported under the auspices of the U. S. Department of Energy by the University of California Lawrence Livermore National Laboratory under contract N° W-7405-Eng-48. This work is supported by the Yucca Mountain Project, LLNL, which is part of the Office of Civilian Radioactive Waste Management (OCRWM-DOE).

References

[1].DOE (2001) "Yucca Mountain Science and Engineering Report," U. S. Department of Energy, Office of Civilian Radioactive Waste Management, DOE/RW-0539, Las Vegas, NV, May 2001.

[2].Gordon, G. M. (2002), "F.N.Speller Award Lecture: Corrosion Considerations Related to Permanent Disposal of High-Level Radioactive Waste"Corrosion, 58, 811 (2002).

[3]. Nuclear Energy Agency (2003), "Engineered Barrier Systems and the Safety of Deep Geological Repositories," Organization for Economic Co-Operation and Development (OECD Publications, 2003: Paris, France).

[4]. McCright, R. D. and H. Weiss, H. (1985), "Corrosion Behavior of Carbon Steels Under Tuff Repository Environmental Conditions," Vol. 44, p 287–294 (Materials Research Society, 1985: Warrendale, PA).

[5].Gdowski, G. E. and Estill, J. C. (1996), "The effect of Water Vapor on the Corrosion of Carbon Steel at 65°C," Vol. 412, p 533–538 (Materials Research Society, 1996: Warrendale, PA).

[6]. T. Lian, D.A. Jones. "Electrochemical Corrosion Behavior of Low Carbon Steel in Concentrated Geologic Vadose Waters" Corrosion, Vol. 55, No.11. p.1012-1019, 1999.[7].Cragnolino, G. A. (1998), Dunn, D. S., Angell, P., Pan, Y.-M. and Sridhar, N., "Factors Influencing the Performance of Carbon Steel Overpacks in the Proposed High-Level Nuclear Waste Repository," Corrosion/98, paper 98147 (NACE International, 1998: Houston, TX).

[8].Brossia, C. S. and Cragnolino, G. A. (1999), "Localized Corrosion of Carbon Steel Outer Overpacks for Nuclear Waste Disposal," Corrosion/99, paper 99468 (NACE International, 1999: Houston, TX).

[9].Scully, J.R. (2003), "The Polarization Resistance Method for determination of Instantaneous Corrosion Rates," Electrochemical Techniques in Corrosion Science and Engineering, p.125-150, 2003. Marcel-Dekker Inc: New York, NY.

[10]. D.C.Silverman, "Primer on the AC Impedance Technique", Electrochemical Techniques for Corrosion Engineering, NACE publication, p.73-79, 1986.

[11]D.A.Jones, "Principles and Preventions of Corrosion",p.162-165,1996. Second Edition, Prentice-Hall Inc.Saddle River, NJ.

[12]. F.Mansfeld, S.Tsai, Corrosion Science, Vol.20, p.853-873, 1979.

[13]. B.W.Lifka,F.L.McGeary, “Corrosion Basics-An Introduction” Chapter 14, Testing and Inspection. P.309-336, Nace Publication,1984.

Table 1. Chemical composition of MCS rock bolt; Balance:Fe

Element	C	Mn	S	Si	Cu	Ni	Cr	Mo	P
% amount	0.44	1.57	0.31	0.27	0.19	0.06	0.08	0.03	0.013

Table 2. Yucca Mountain Water(1X) chemical composition; pH: 8.3

Ions	Na^+	SiO_2	Ca^{2+}	K^+	Mg^{2+}	$HCO3^-$	Cl^-	$SO4^{2-}$	F^-
mg/L	61.3	70.5	101	8.0	17.0	200	117	116	0.86

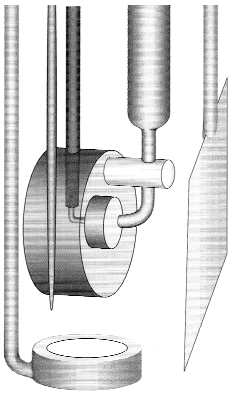

Figure 1. Arrangement of the cell elements used for potentiodynamic scanning and EIS techniques for corrosion rate determination of MCS in YM waters.

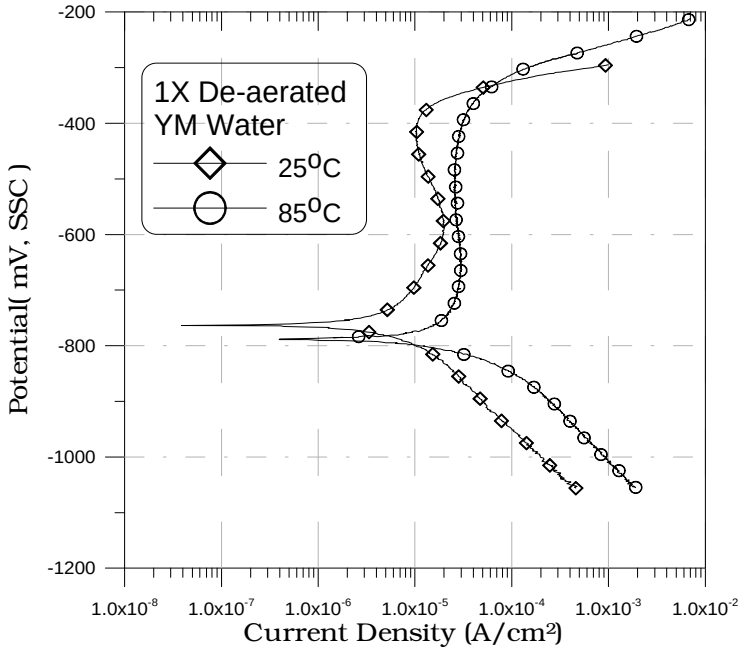

Figure 2. Temperature effect on Corrosion of MCS: Potentiodynamic linear polarization behavior in the de-aerated simulated 1X YM waters at 25°C and 85°C.

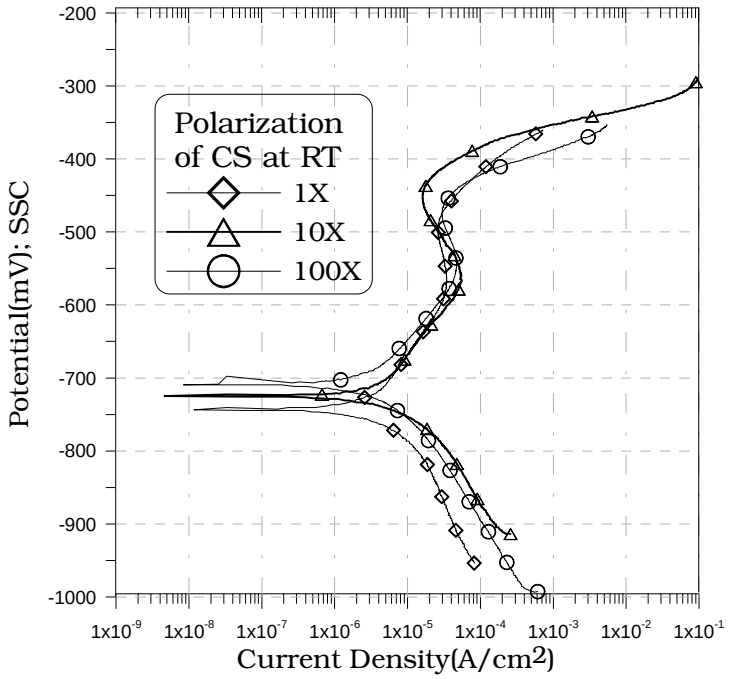

Figure 3.Concentration Effect on Corrosion of MCS: Potentiodynamic linear polarization behavior of various concentrations in the de-aerated simulated waters at 25°C .

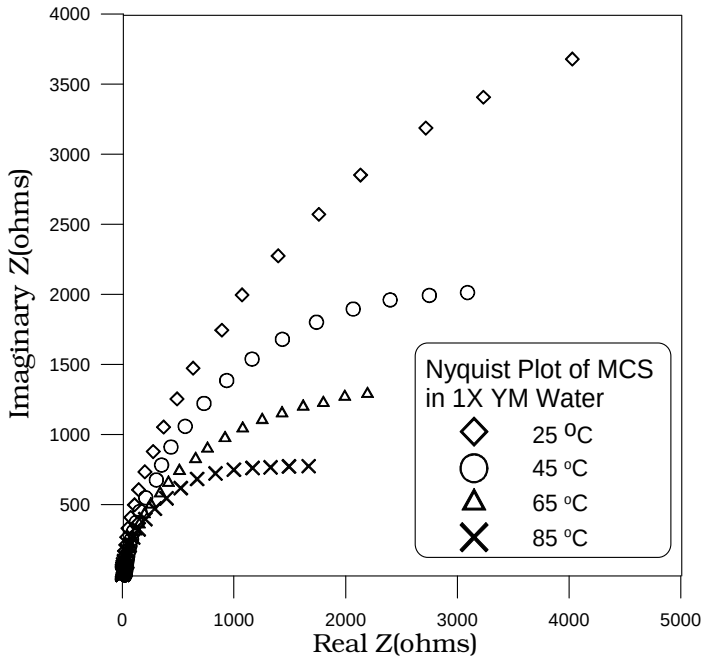

Figure 4. Temperature Effect: Nyquist plots from the Electrochemical impedance spectroscopy at E_{corr}, in deaerated 1x YM waters of for various temperatures.

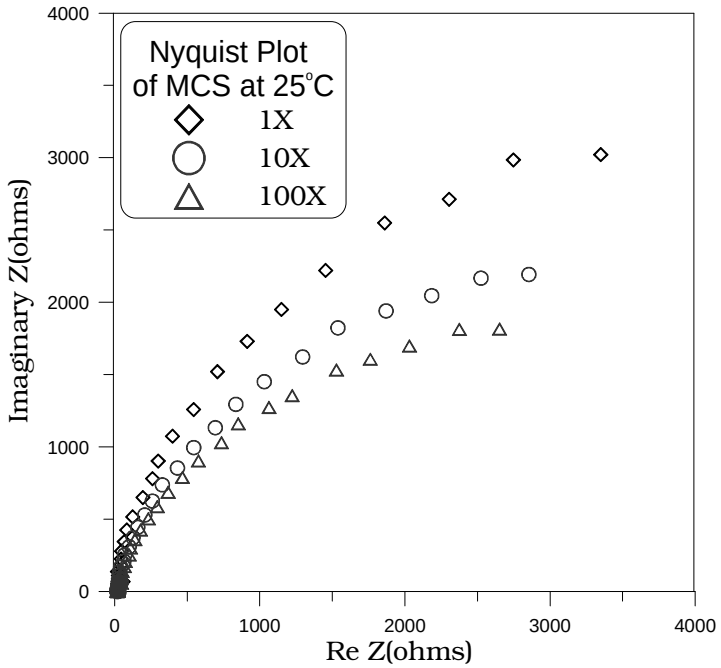

Figure 5. Concentration Effect: Nyquist plots from the Electrochemical impedance spectroscopy at E_{corr}, for various concentrations of de-aerated YM waters at 25°C.

Table 3. Corrosion rates of MCS rock bolt by the polarization resistance technique in the concentrated de-aerated YM Waters.

	Concentration (times)	Temperature (^oC)	Icorr (A/cm^2)	Corrosion Rates (mils/year)	(mμ/year)
Deaerated	1X	25	3.8x10-6	1.7	45
		45	6.0x10-6	2.7	70
		65	1.0x10-5	4.7	120
		85	1.3x10-5	6.3	160
	10X	25	3.0x10-6	1.4	35
		45	5.5x10-6	2.3	58
		65	1.0x10-5	4.6	116
		85	1.4x10-5	6.4	162
	100X	25	4.5x10-6	2.0	51
		45	6.0x10-6	2.7	68
		65	1.0x10-5	4.5	113
		85	1.5x10-5	6.7	168

Table 4. Corrosion rates of MCS rock bolt by the polarization resistance technique in the concentrated aerated YM Waters.

	Concentration (times)	Temperature (^oC)	I_{corr} (A/cm^2)	Corrosion Rates (mils/year)	(mμ/year)
Aerated	1X	25	$1.1x10^{-5}$	4.9	124
		45	$2.8x10^{-5}$	12.6	320
		65	$5.6x10^{-5}$	24.8	630
		85	$1.0x10^{-4}$	45.0	1134
	10X	25	$1.2x10^{-5}$	5.4	136
		45	$3.5x10^{-5}$	16.0	396
		65	$6.6x10^{-5}$	30.0	750
		85	$9.4x10^{-5}$	42.0	1058
	100X	25	$2.0x10^{-5}$	9.0	226
		35	$3.9x10^{-5}$	18.0	446
		45	$4.5x10^{-5}$	20.0	510
		55	$3.3x10^{-5}$	15.0	378
		65	$2.3x10^{-5}$	10.3	261
		75	$1.8x10^{-5}$	7.9	199
		85	$1.7x10^{-5}$	7.6	193

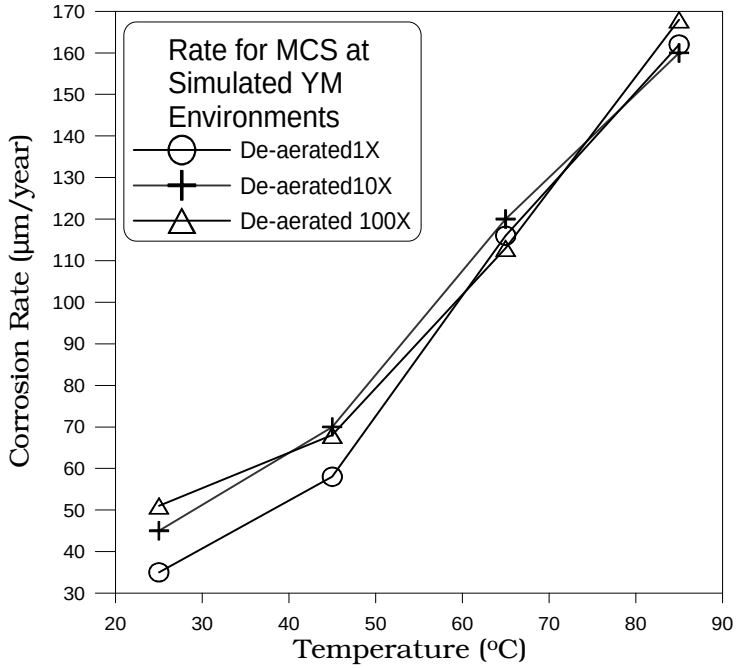

Figure 6. Temperature effect on corrosion rates of MCS rock bolt in simulated de-aerated concentrated YM waters by polarization resistance technique.

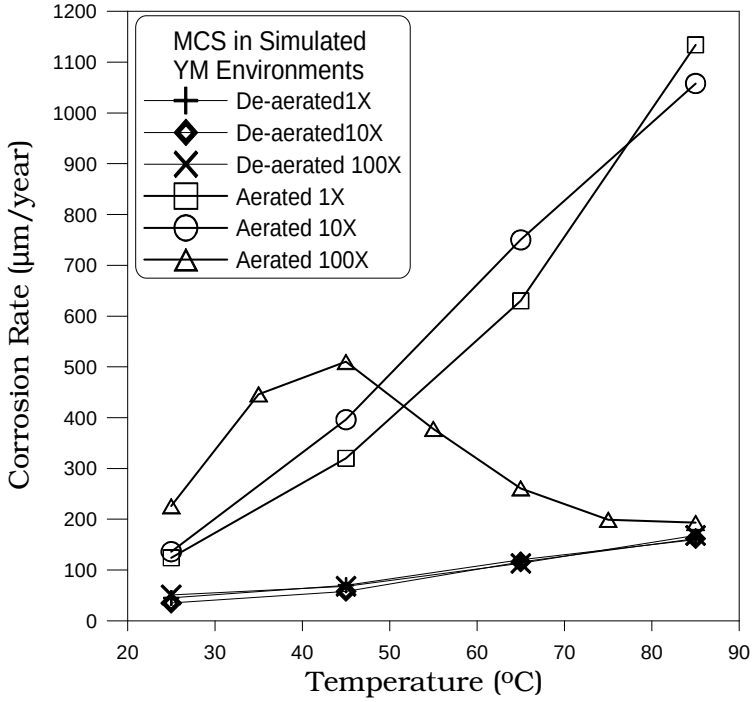

Figure 7. Temperature effect on corrosion rates of MCS rock bolt in aerated and de-aerated concentrated YM waters by polarization resistance technique.

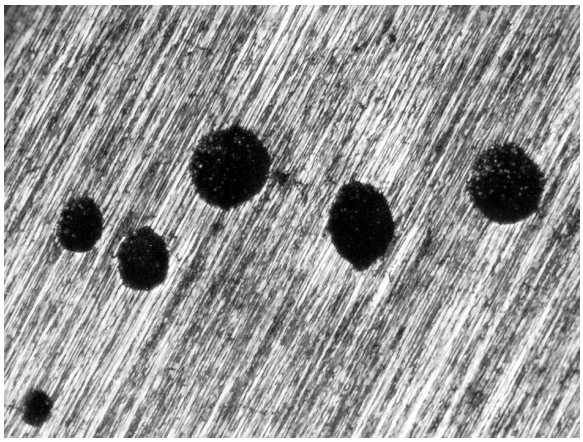

Figure 8. Protective film formation and pitting over the MCS rock bolt in the de-aerated 100X YM waters at 85^{o}C after anodic polarization.

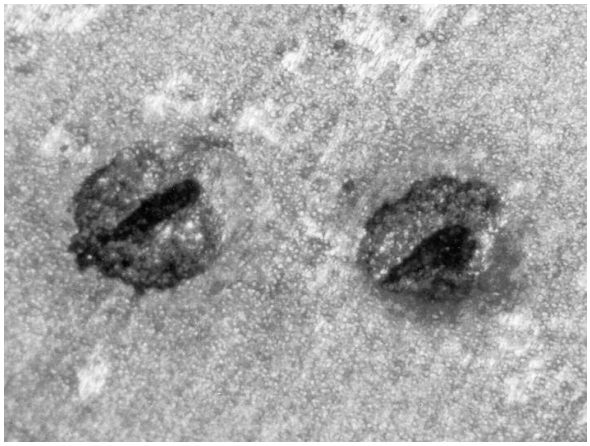

Figure 9. Protective film formation and pitting over the MCS rock bolt in the aerated 100X YM waters at 85^{o}C after anodic polarization.

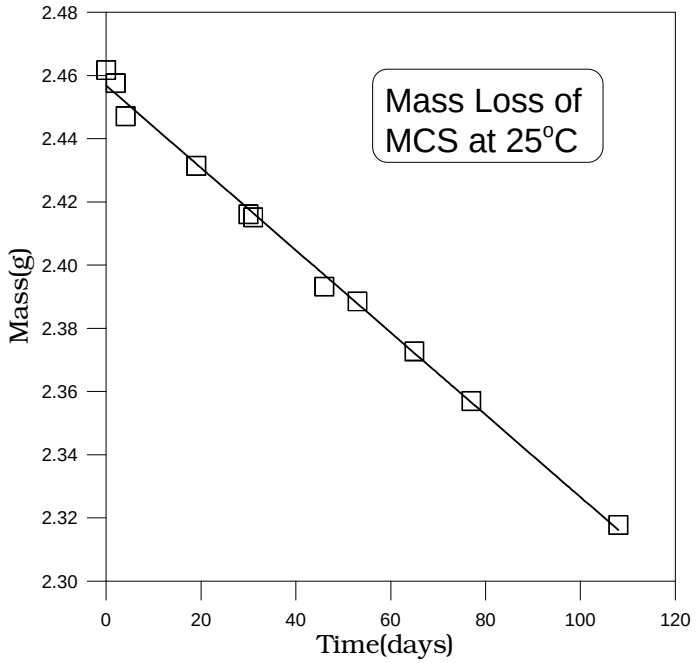

Figure 10. Mass loss profile of fully immersed MCS rock bolt in the 1X YM water at 25°C

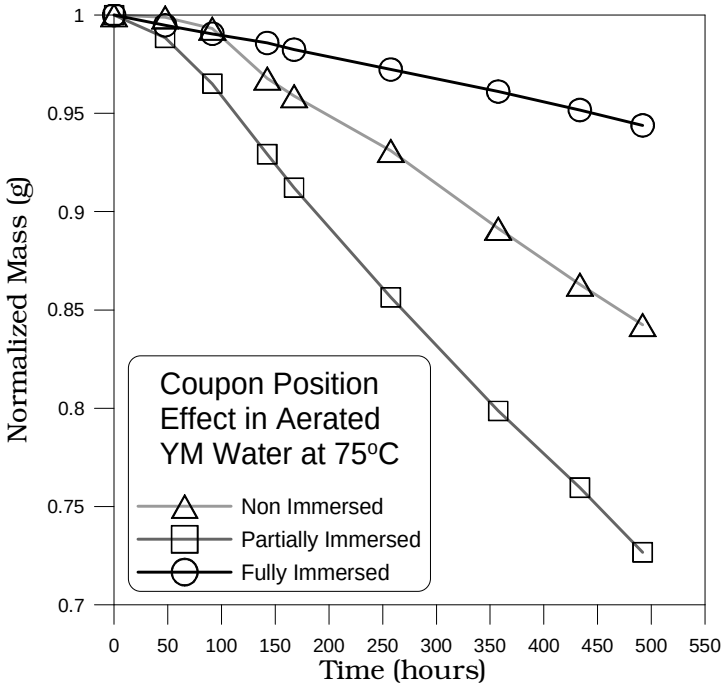

Figure 11. Lab immersion corrosion testing in 1X YM water at 75°C with three different coupon positions such as total immersion, partial immersion, and vapor immersion (in the humid part above the water line)

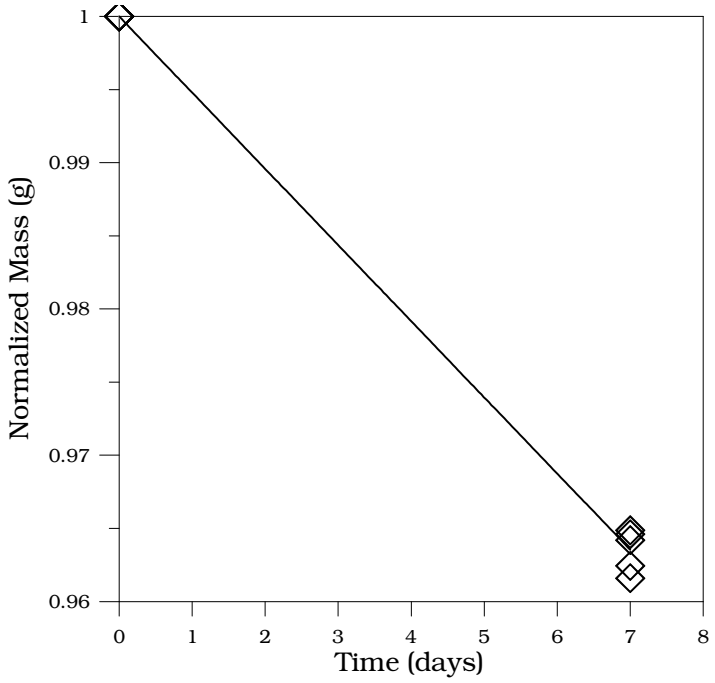

Figure 12. Mass loss of MCS rock bolt in YM spray environment at 35°C.

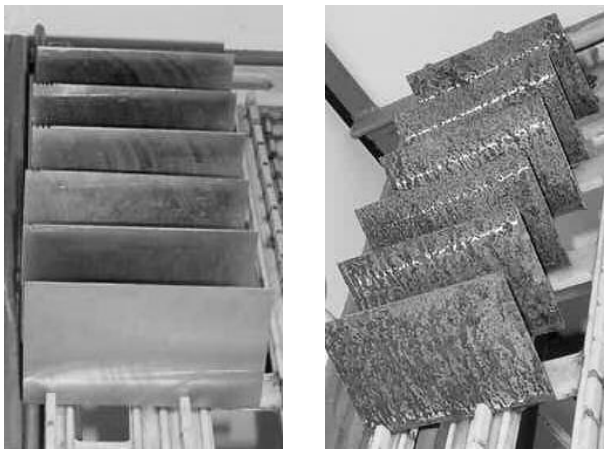

Figure 13. Simulated 1X YM water spray test coupons, before and after the exposure tests at 35°C.